Supplementary Information

Chameleonic layered metal-organic frameworks with variable charge-ordered states triggered by temperature and guest molecules

Jian Chen,[a,b] Yoshihiro Sekine,[a,b] Atsushi Okazawa,[c] Hiroyasu Sato,[d] Wataru Kosaka,[a,b] and Hitoshi Miyasaka*[a,b]

[a] Institute for Materials Research, Tohoku University,
2–1–1 Katahira, Aoba-ku, Sendai 980-8577, Japan
E-mail: miyasaka@imr.tohoku.ac.jp

[b] Department of Chemistry, Graduate School of Science, Tohoku University,
6–3 Aramaki-Aza-Aoba, Aoba-ku, Sendai 980-8578, Japan

[c] Department of Basic Science, Graduate School of Arts and Sciences, The University of Tokyo,
3–8–1 Komaba, Meguro-ku, Tokyo 153-8902, Japan

[d] Application Laboratory, Rigaku Corporation,
3–9–12, Matsubara-cho, Akishima-shi, Tokyo 196-8666, Japan

Experimental Section

General Considerations. All the reagents and solvents were purchased from commercial sources and used without any further purification. The fresh compound $(NPr_4)_2[Fe_2(Cl_2An)_3]\cdot 2(acetone)\cdot H_2O$ (**1**) was synthesized according to the previous literature method.[1]

Preparation of $(NPr_4)_2[Fe_2(Cl_2An)_3]$ (**1-d**).

The crystallization lattice solvents, 2(acetone)·(H_2O), in **1** could be removed by evacuating for 12 hours at room temperature to form the desolvated compound **1-d**. Elemental analysis (%) was calculated for $C_{42}H_{56}Cl_6Fe_2N_2O_{12}$: C 45.64, H 5.11, and N 2.53. Measured values (%) were found: C 45.25, H 5.02, and N 2.59.

Preparation of $(NPr_4)_2[Fe_2(Cl_2An)_3]\cdot 2(acetone)\cdot H_2O$ (**1'**).

Exposing a polycrystalline sample of **1-d** in a vapor of a mixed solution of acetone and water (2:1 vol%) for more than two hours formed a crystal sample of **1'**. Elemental analysis (%) was calculated for $C_{48}H_{70}Cl_6Fe_2N_2O_{15}$: C 46.51, H 5.69, and N 2.26. Measured values (%) were found: C 46.71, H 5.58, and N 2.18.

X-ray Crystallographic Analysis. Single-crystal X-ray diffraction (SC-XRD) analysis data measured at several temperatures below 300 K for **1-d** and **1'** were recorded on a charge-coupled device (CCD) diffractometer (Rigaku Saturn 724) with multilayer mirror monochromated Mo Kα radiation (λ = 0.71073 Å). A single crystal was mounted on a thin Kapton film using Nujol and cooled under N_2 for the measurements below 300 K. SC-XRD analysis data at T =335 K and 380 K, as well as at 300 K, for **1-d** were collected on a Rigaku XtaLAB Synergy diffractometer using multi-layer mirror monochromated Cu-Kα radiation (λ = 1.54184 Å). The structures were solved using direct methods (SHELXT Version 2014/5) for which were expanded using Fourier techniques. All calculations except for refinement were performed using the Crystal Structure crystallographic software package, and the refinement was performed using SHELXL Version 2014/7.[2] X-ray crystallographic data for **1-d** at 103 K (CCDC-1971740), 300 K (CCDC-1971741), 330 K (CCDC-1971742), and 380 K (CCDC-1971743) (CIF) can be obtained free of charge from the Cambridge Crystallographic Data Centre via https://www.ccdc.cam.ac.uk/structures/. Please contact the corresponding author if the structural information of **1'** (103 K) and **1-d** (242 K, 289 K, 298 K) as crystallographic information file (CIF) format is required. The structural diagrams were prepared using VESTA software.[3] Powder X-ray diffraction (PXRD) patterns were collected for samples at 0.02° steps, filled into a glass capillary (ϕ = 0.5 mm) and installed on a RIGAKU Ultima IV diffractometer, with Cu Kα radiation (λ = 1.5418 Å) at room temperature.

Physical Measurements. Thermally gravimetric analysis (TGA) were recorded on a Shimadzu DTG-60H apparatus under a flowing N_2 atmosphere from 20 to 400 °C at a heating rate of

5 ºC min^{-1}. Differential scanning calorimetry (DSC) data for **1-d** were collected using a Shimadzu DSC-60 instrument at a rate of 5 K min^{-1} under a N_2 atmosphere. Magnetic properties measurements were conducted with a SQUID magnetometer (MPMS-XL, Quantum Design, U.S.A.). Magnetization measurements were performed by applying a 1 kOe DC magnetic field in a temperature range of 1.8–400 K. Field dependence of the magnetization measurements were performed at 1.8 K from −7 to +7 T. AC magnetic measurements were performed at various frequencies ranging from 1 to 1488 Hz with an AC field amplitude of 3 Oe and without application of DC field. *In situ* desolvation/solvation-magnetic measurements were conducted using a home-made closed cell followed by the previous literature.[4] For ^{57}Fe Mössbauer spectroscopic measurement (Topologic Systems Co., Kanagawa, Japan), ^{57}Co in Rh matrix was used as a Mössbauer source. The spectra were calibrated by using the six lines of a body-centered cubic iron foil (α-Fe), the center of which was taken as zero isomer shift. ^{57}Fe Mössbauer spectroscopic measurement at high temperature were performed with home-made cell under a N_2 atmosphere. DC electronic conductivity on a single crystal was measured at a cryostat by a two-probe method with a KEITHLEY 2635A nanovoltmeter, where the contacts were made with gold wires (30 μm of diameter) by using Dotite carbon paint (a graphite emulsion in a mixture of solvents) purchased by Nilaco. The single crystals were hexagonal prisms with typical size of ~ 0.2× 0.1 × 0.2 mm^3 (Fig. S14).

SC-XRD measurements using a synchrotron at SPring-8, Hyogo.

Within the treatments taking a unit cell (2*a*, *b*, 1.5*c* in $P2_1/c$ with $Z = 6$) three times larger than the pristine cell (*a*, *b*, *c* in $P2_1/n$ with $Z = 2$), where all atoms of the unit cell were determined as an asymmetric unit, the observed structure still had an intermediate value between the HT (Fe^{3+}–$L_A{}^{\bullet 3-}$) and LT (Fe^{2+}–$L_A{}^{2-}$) species for all components. This result indicates that the charges of Fe^{n+}–$L_A{}^{m-}$ were disproportionately distributed within each layer with either IM_d (charge-disordered disproportionate state) or IM_o, but not alternating between layers.

Table S1. Crystallographic data for **1’** measured at 103 K, comparing with crystallographic data for **1** obtained from the literature.[1] These data were recorded on a charge-coupled device (CCD) diffractometer (Rigaku Saturn 724) with multilayer mirror monochromated Mo Kα radiation (λ = 0.71073 Å).

Compound	**1**	**1’**
Temperature / K	103	103
Formula	$C_{48}H_{70}Cl_6Fe_2N_2O_{15}$	$C_{48}H_{70}Cl_6Fe_2N_2O_{15}$
Formula Weight	1239.50	1239.50
Habit	hexagonal	hexagonal
Crystal System	monoclinic	monoclinic
Space group	$P2_1/c$	$P2_1/c$
a / Å	20.1956(4)	20.115(3)
b / Å	21.8021(5)	21.943(2)
c / Å	14.4138(3)	14.3614(14)
β / °	108.127(2)	107.791(13)
V / Å^3	6031.5(2)	6035.7(13)
Z	4	4
Crystal size / mm^3	0.133 × 0.118 × 0.027	0.165 × 0.120 ×0.033
D_{calc} / g cm^{-3}	1.365	1.364
F_{000}	2584.00	2584.00
λ / Å	0.71073	0.71073
μ(Mo Kα) / cm^{-1}	8.061	8.056
Data measured	48919	43466
Data unique	13808	12442
R_{int}	0.0332	0.1412
No. of observations	13808	12442
No. of variables	667	667
$R1$ ($I > 2.00\sigma(I)$)^a	0.0444	0.1707
R (all reflections)^a	0.0634	0.2883
$wR2$ (All reflections)^b	0.1288	0.4412
GOF	1.034	1.031

a) $R1 = R = \sum||F_o| - |F_c||/\sum|F_o|$. *b*) $wR2 = [\sum w(F_o^2 - F_c^2)^2)/\sum w(F_o^2)^2]^{1/2}$.

Table S2. Crystallographic data for **1-d** measured at $T < 300$ K, recorded on a charge-coupled device (CCD) diffractometer (Rigaku Saturn 724) with multilayer mirror monochromated Mo Kα radiation ($\lambda = 0.71073$ Å).

Temperature / K	103	242	289	298
Formula	$C_{42}H_{56}Cl_6Fe_2N_2O_{12}$	$C_{42}H_{56}Cl_6Fe_2N_2O_{12}$	$C_{42}H_{56}Cl_6Fe_2N_2O_{12}$	$C_{42}H_{56}Cl_6Fe_2N_2O_{12}$
Formula Weight	1105.32	1105.32	1105.32	1105.32
Habit	hexagonal	hexagonal	hexagonal	hexagonal
Crystal System	monoclinic	monoclinic	monoclinic	monoclinic
Space group	$P2_1/n$	$P2_1/n$	$P2_1/n$	$P2_1/n$
a / Å	10.7583(4)	10.8331(7)	10.8746(7)	10.8817(8)
b / Å	20.7341(5)	20.8828(10)	20.9268(11)	20.9433(12)
c / Å	12.2345(5)	12.2513(8)	12.2581(8)	12.2635(8)
β / °	101.160(4)	101.717(6)	101.889(6)	101.938(7)
V / Å^3	2677.47(17)	2713.8(3)	2729.7(3)	2734.4(3)
Z	2	2	2	2
Crystal size / mm^3	0.168 × 0.162 × 0.061	0.168 × 0.162 × 0.061	0.168 × 0.162 × 0.061	0.168 × 0.162 × 0.061
D_{calc} / g cm^{-3}	1.371	1.353	1.345	1.342
F_{000}	1144.00	1144.00	1144.00	1144.00
λ / Å	0.71073	0.71073	0.71073	0.71073
μ(Mo Kα) / cm^{-1}	8.949	8.829	8.778	8.763
Data measured	20842	21277	21510	21515
Data unique	6114	6194	6244	6255
R_{int}	0.0309	0.0444	0.0483	0.0507
No. of observations	6114	6194	6244	6255
No. of variables	289	289	289	289
$R1$ ($I > 2.00\sigma(I)$)^a	0.0413	0.0506	0.0569	0.0571
R (all reflections)^a	0.0566	0.0845	0.1009	0.1083
$wR2$ (All reflections)^b	0.0959	0.1118	0.1182	0.1223
GOF	1.084	1.036	1.031	1.009
CCDC No.	1971740	–	–	–

a) $R1 = R = \sum||F_o| - |F_c||/\sum|F_o|$. *b*) $wR2 = [\sum w(F_o^2 - F_c^2)^2)/\sum w(F_o^2)^2]^{1/2}$.

Table S3. Selected bond lengths (Å) in the Cl_2An moieties and around the Fe centers in **1-d** in the temperature range from 103 K to 298 K.

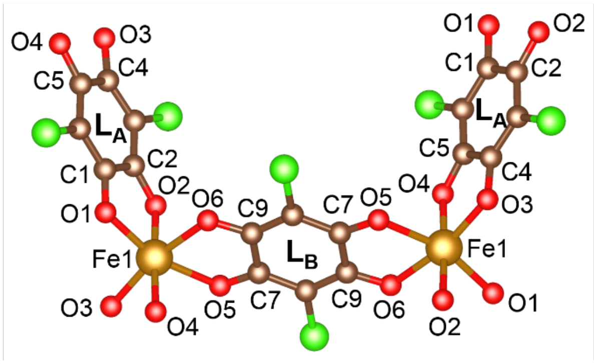

Temperature / K	103	242	289	298
Fe1-O1	1.9777(16)	1.983(2)	1.991(2)	1.988(2)
Fe1-O2	1.9928(16)	1.9967(19)	1.998(2)	1.999(2)
Fe1-O3	1.9842(16)	1.988(2)	1.987(2)	1.993(2)
Fe1-O4	1.9957(16)	1.998(2)	1.998(2)	2.003(2)
Fe1-O5	2.0772(17)	2.081(2)	2.085(2)	2.085(2)
Fe1-O6	2.0872(17)	2.088(2)	2.090(2)	2.093(2)
C1-O1	1.295(3)	1.292(3)	1.293(3)	1.289(3)
C2-O2	1.290(3)	1.289(3)	1.288(4)	1.286(4)
C4-O3	1.298(3)	1.294(3)	1.293(3)	1.294(3)
C5-O4	1.288(3)	1.287(3)	1.290(4)	1.284(4)
C7-O5	1.262(3)	1.261(4)	1.260(4)	1.261(4)
C9-O6	1.252(3)	1.256(4)	1.253(4)	1.255(4)

Table S4. Crystallographic data for **1-d** measured at $T \geq 300$ K, collected on a Rigaku XtaLAB Synergy diffractometer using multi-layer mirror monochromated Cu-Kα radiation ($\lambda = 1.54184$ Å).

Temperature / K	300	335	380
Formula	$C_{42}H_{56}Cl_6Fe_2N_2O_{12}$	$C_{42}H_{56}Cl_6Fe_2N_2O_{12}$	$C_{42}H_{56}Cl_6Fe_2N_2O_{12}$
Formula Weight	1105.32	1105.32	1105.32
Habit	hexagonal	hexagonal	hexagonal
Crystal System	monoclinic	monoclinic	monoclinic
Space group	$P2_1/n$	$P2_1/n$	$P2_1/n$
a / Å	10.8740(9)	10.8660(10)	10.9375(9)
b / Å	20.9284(16)	21.1945(18)	21.2780(15)
c / Å	12.2372(8)	12.2707(9)	12.2835(7)
β / °	101.859(7)	101.413(8)	100.818(6)
V / Å^3	2725.4(4)	2770.1(4)	2807.9(3)
Z	2	2	2
Crystal size / mm^3	0.383 × 0.237 × 0.127	0.383 × 0.237 × 0.127	0.383 × 0.237 × 0.127
D_{calc} / g cm^{-3}	1.347	1.325	1.307
F_{000}	1144.00	1144.00	1144.00
λ / Å	1.54184	1.54184	1.54184
μ(Cu Kα) / cm^{-1}	74.317	73.120	72.135
Data measured	16308	16591	16374
Data unique	4950	5042	5114
R_{int}	0.0735	0.0986	0.0975
No. of observations	4950	5042	5114
No. of variables	293	293	293
$R1$ ($I > 2.00\sigma(I)$)^a	0.0639	0.0699	0.0743
R (all reflections)^a	0.1177	0.1498	0.1831
$wR2$ (All reflections)^b	0.1899	0.2218	0.2334
GOF	1.012	0.982	0.996
CCDC No.	1971741	1971742	1971743

a) $R1 = R = \sum\|F_o| - |F_c\|/\sum|F_o|$. *b*) $wR2 = [\sum w(F_o^2 - F_c^2)^2)/\sum w(F_o^2)^2]^{1/2}$.

Table S5. Selected bond lengths (Å) in the Cl_2An moieties and around the Fe centers in **1-d** in the temperature range from 300 K to 380 K.

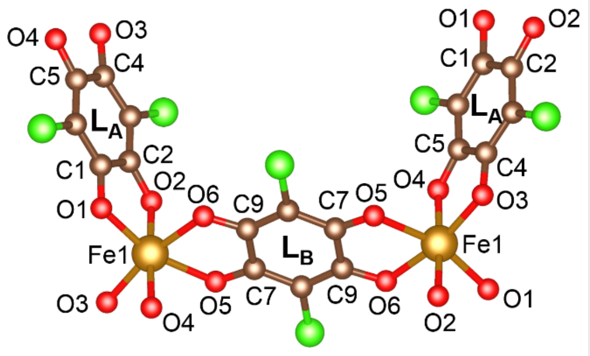

Temperature / K	300	335	380
Fe1-O1	1.989(3)	2.032(4)	2.085(4)
Fe1-O2	2.005(3)	2.050(4)	2.103(4)
Fe1-O3	1.992(3)	2.041(4)	2.085(4)
Fe1-O4	2.000(3)	2.048(4)	2.095(4)
Fe1-O5	2.083(4)	2.082(5)	2.101(5)
Fe1-O6	2.091(4)	2.093(5)	2.108(5)
C1-O1	1.284(5)	1.268(6)	1.250(7)
C2-O2	1.293(6)	1.267(7)	1.253(8)
C4-O3	1.283(5)	1.280(6)	1.254(7)
C5-O4	1.286(6)	1.270(7)	1.249(8)
C7-O5	1.261(6)	1.265(9)	1.277(10)
C9-O6	1.258(6)	1.245(9)	1.239(11)

Table S6. ^{57}Fe Mössbauer parameters for **1-d** measured at 300, 335, and 380 K.

Temp. (K)	δ (mm s^{-1})			ΔE_Q (mm s^{-1})			Area (%)		
	Fe^{II}_{HS}	Fe^{III}_{HS}	impurity	Fe^{II}_{HS}	Fe^{III}_{HS}	impurity	Fe^{II}_{HS}	Fe^{III}_{HS}	impurity
300	-	0.500(2)	-	-	1.228(5)	-	-	100.0	-
335	0.968(9)	0.463(4)	0.299(14)	1.152(17)	1.164(8)	0.57(3)	38.5	38.5	23.0
380	1.021(11)	-	0.250(19)	0.83(2)	-	0.51(3)	56.5	-	43.5

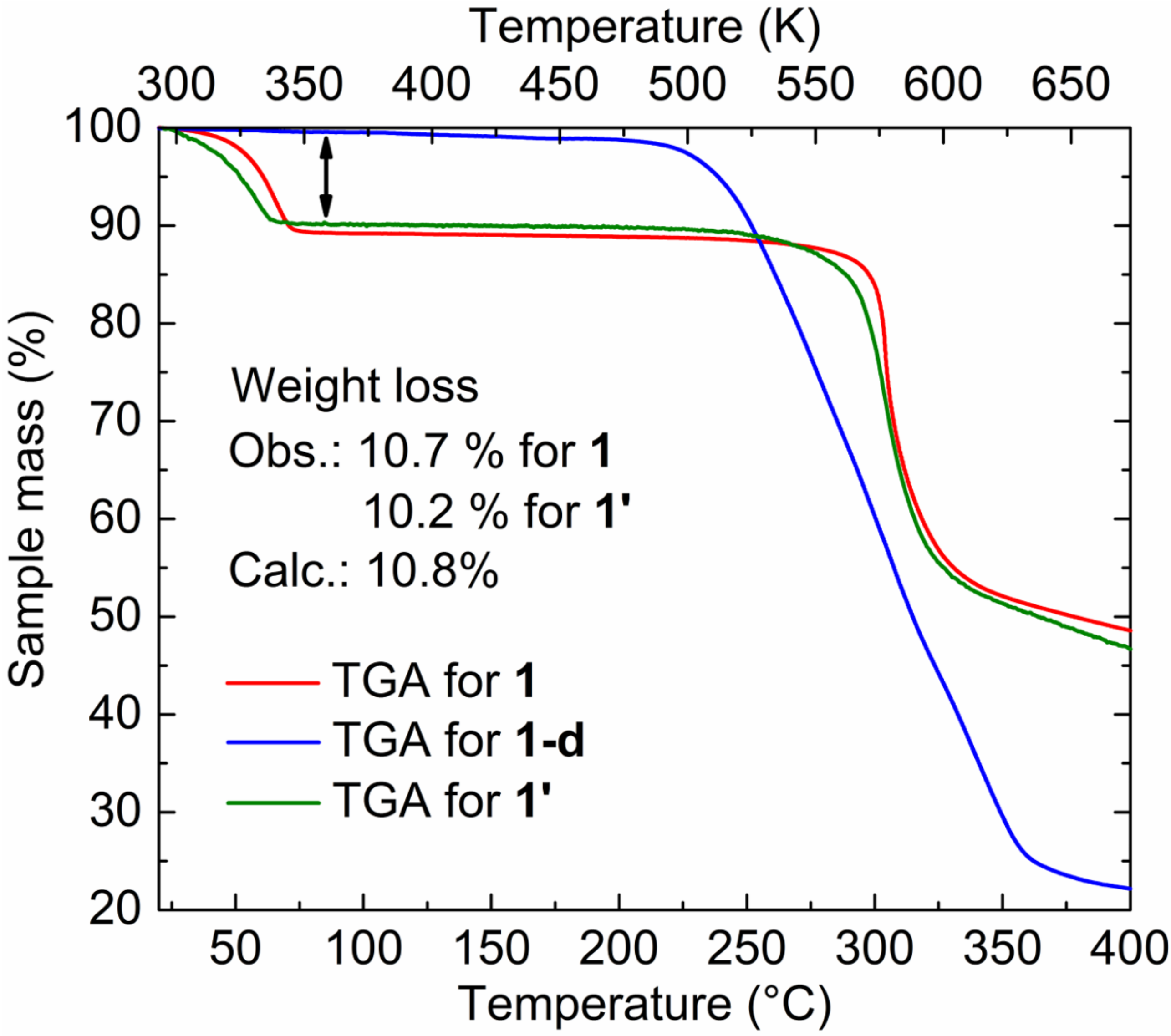

Fig. S1. Thermally gravimetric analysis (TGA) profiles of **1** (red),[1] **1-d** (blue), and **1'** (green) with a heating rate of 5 °C min^{-1}. The calculated weight loss value 10.8 % indicates the percentage for crystallization solvent of 2(acetone)·H_2O.

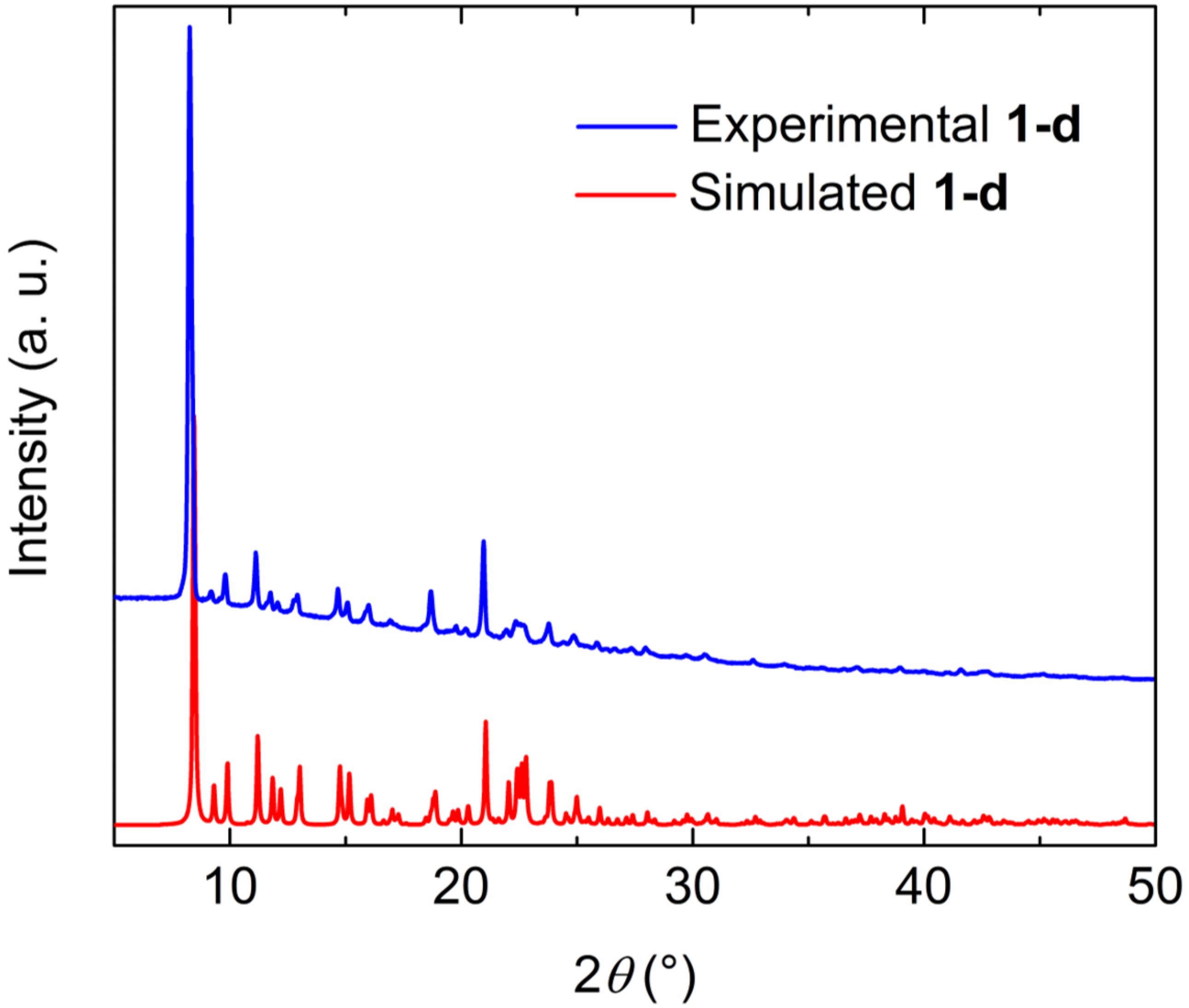

Fig. S2. Experimental and simulated X-ray powder diffractograms for **1-d** at room temperature.

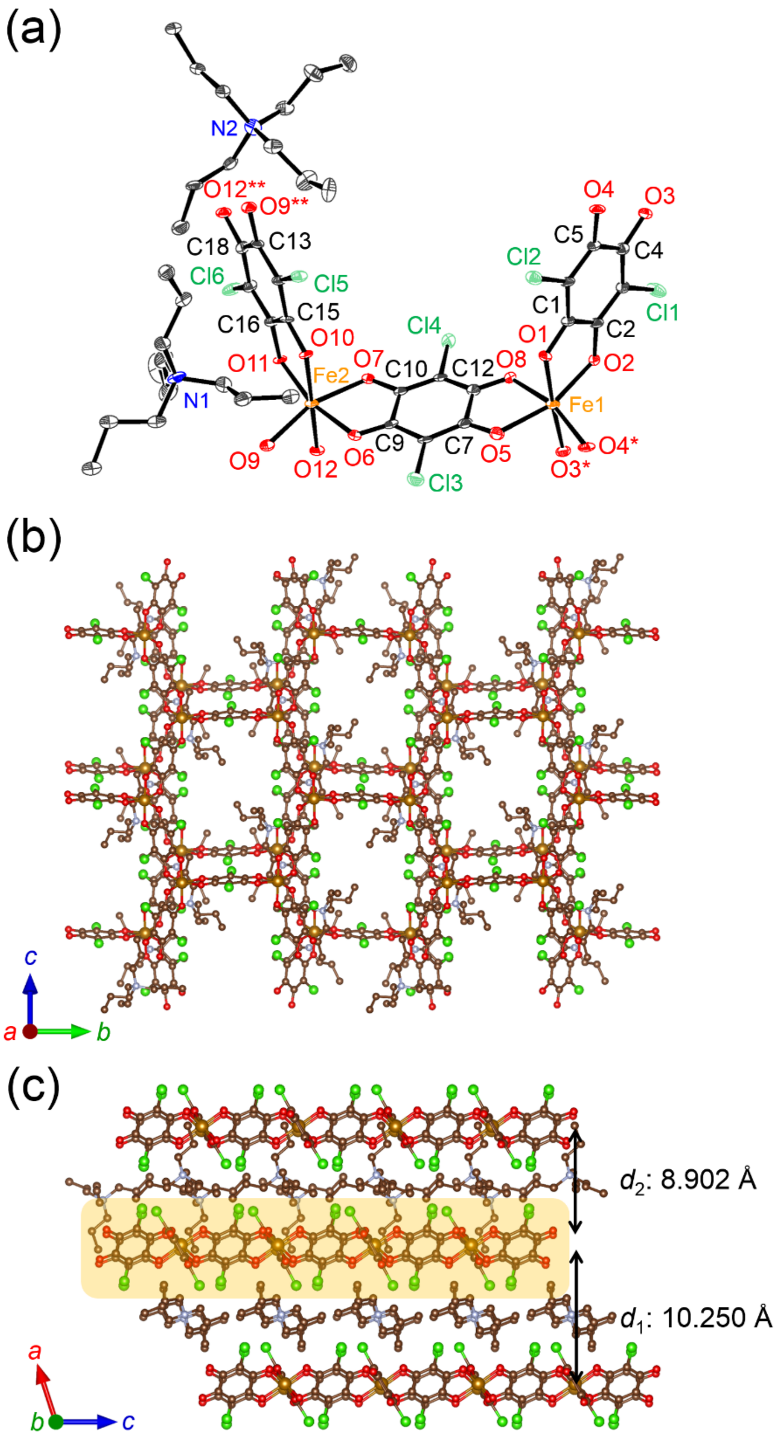

Fig. S3. Crystal Structure of **1'**. (a) Thermal ellipsoid plot of the formula unit of **1'** with the atomic numbering scheme at 103 K, where Fe, O, C, Cl, and N are represented in orange, red, black, green, and blue, respectively. Symmetry operations: (*) *x*, 3/2−*y*, 1/2+*z*; (**) *x*, 1/2−*y*, −1/2+*z*. (b), and (c) show the packing structures of alternating anionic layers of $[Fe_2(Cl_2An)_3]^{2-}$ and NPr_4^+ cations in **1'**, projecting along the crystallographic *a*-axis and *b*-axis, respectively. Fe, C, O, Cl, and N atoms are represented in orange, brown, red, green, and light blue, respectively. One of the anionic layers was highlighted by pale-yellow band. Crystallization solvents (acetone and water molecules) and hydrogen atoms are omitted for clarity.

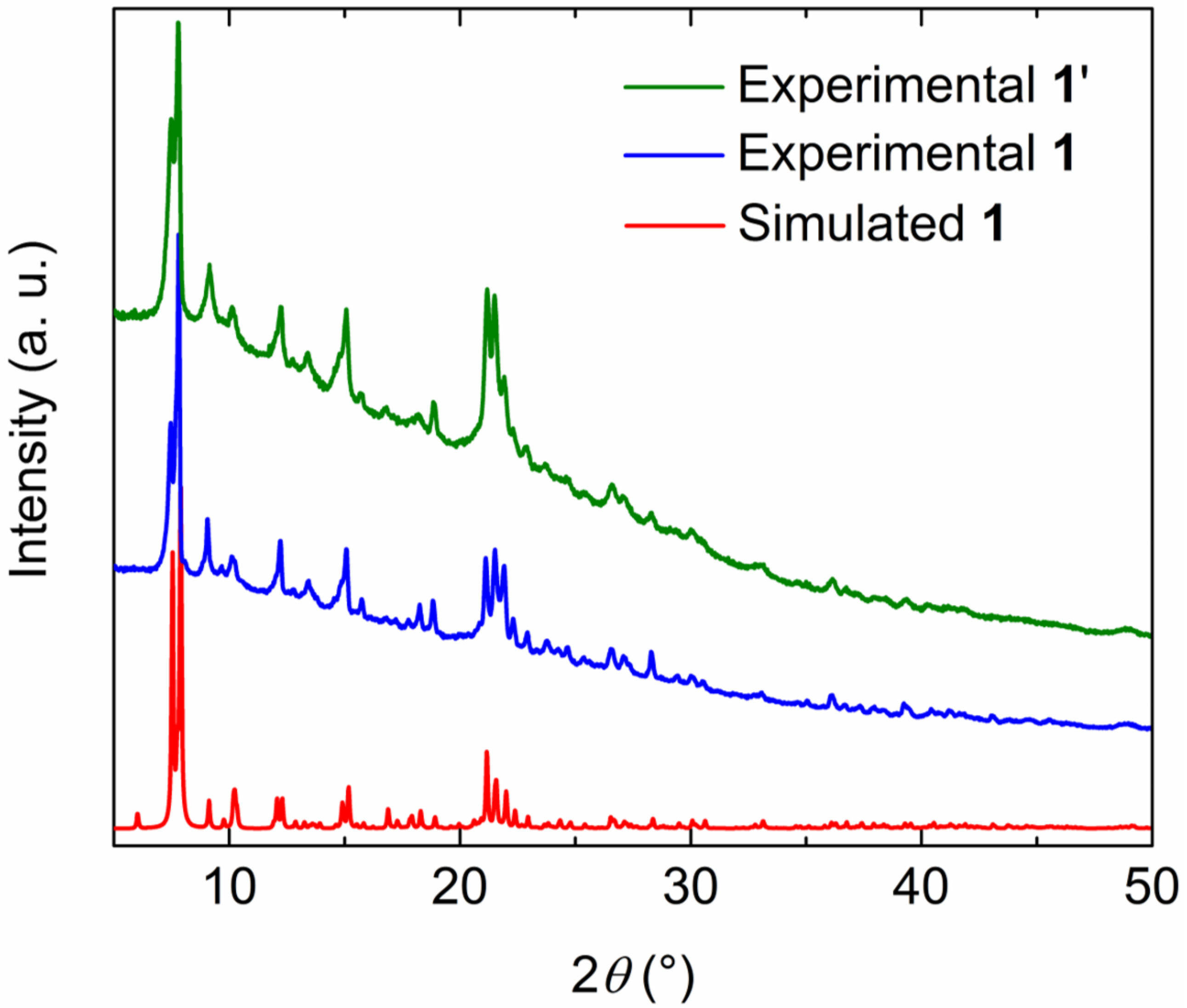

Fig. S4. Experimental X-ray powder diffractograms for **1** (blue)[1] and **1'** (green) measured at room temperature, and simulated X-ray powder diffractogram for **1** (red) was obtained from literature.[1]

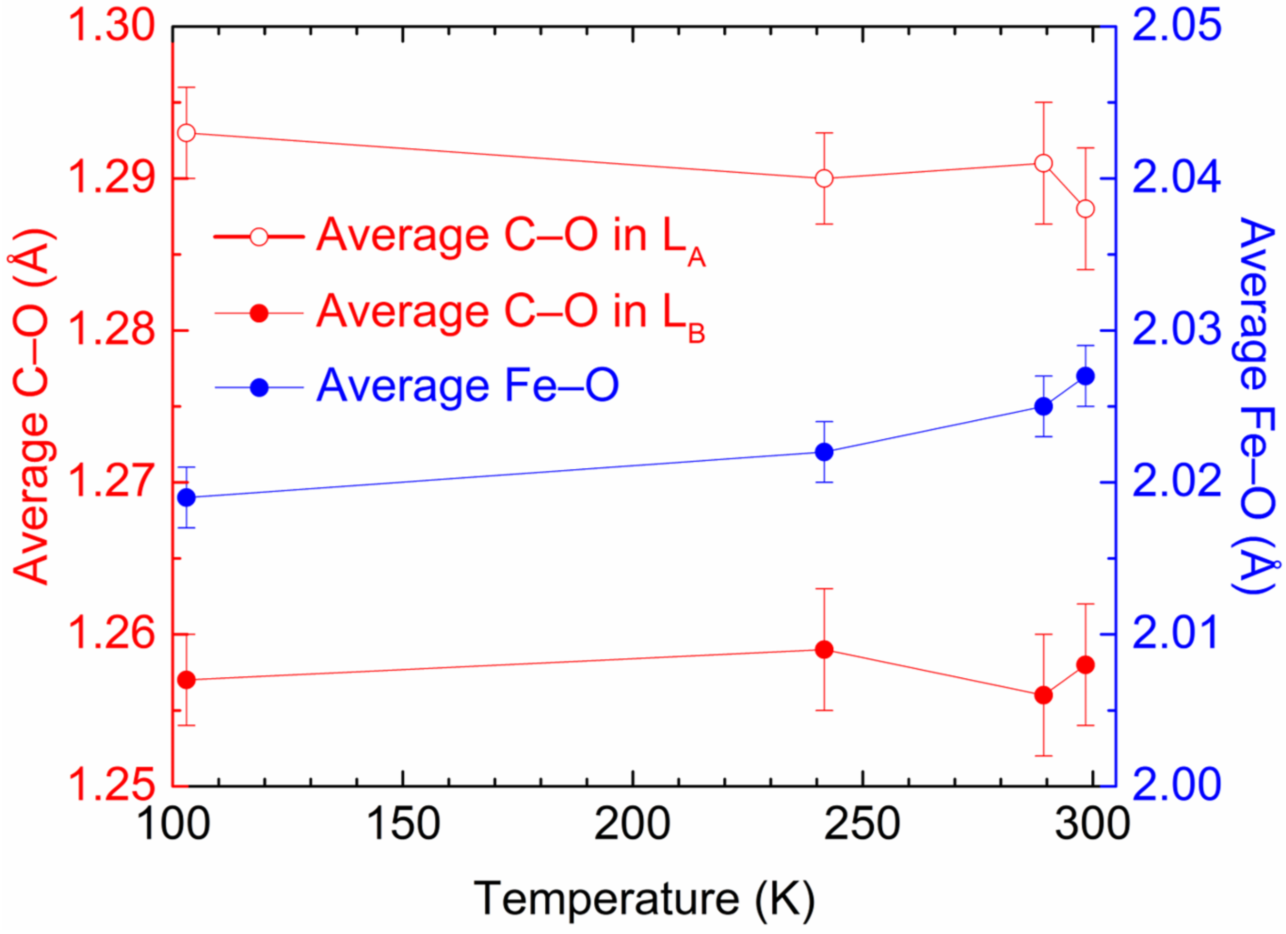

Fig. S5. Temperature dependence of average bond lengths in Cl_2An^{m-} moieties and around a coordinating Fe center in **1-d**, where the bond lengths were obtained from single-crystal X-ray crystallography at each temperature. The red open, red closed and blue closed circles represent the average C–O bond lengths of L_A, L_B and average Fe–O bond lengths around Fe ions.

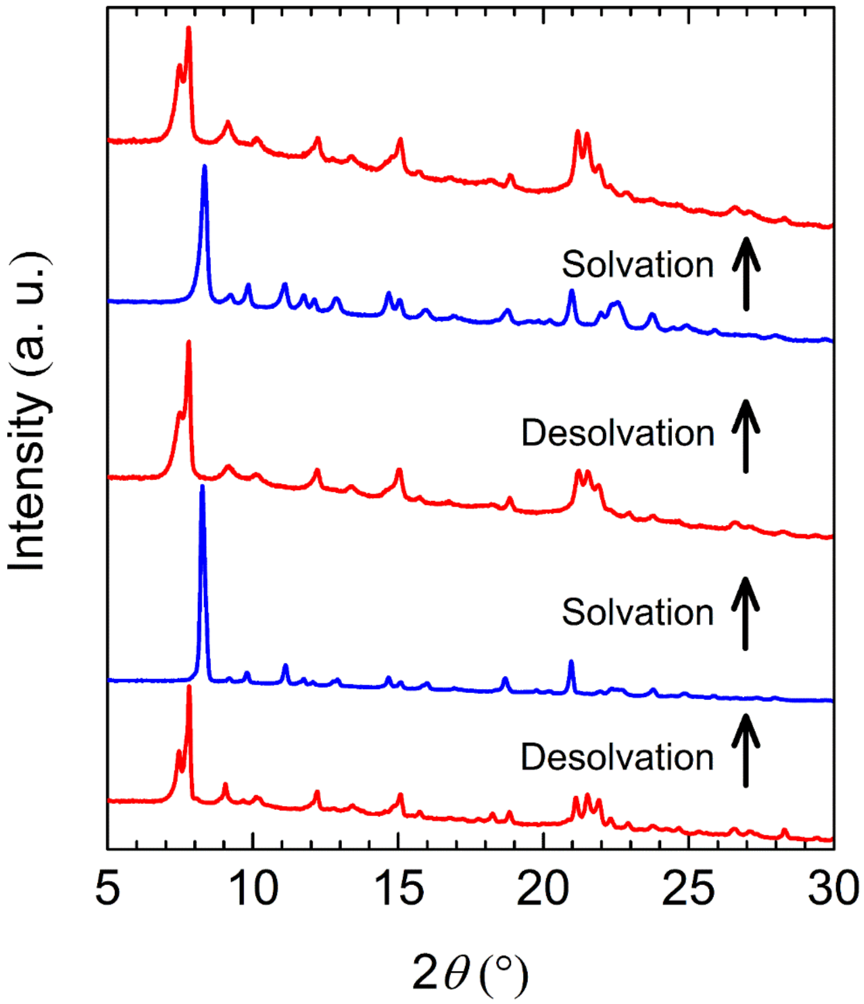

Fig. S6. Variation of PXRD patterns between solvated phase (**1**/**1’**) and desolvated phase (**1-d**) during desolvation/solvation cycles.

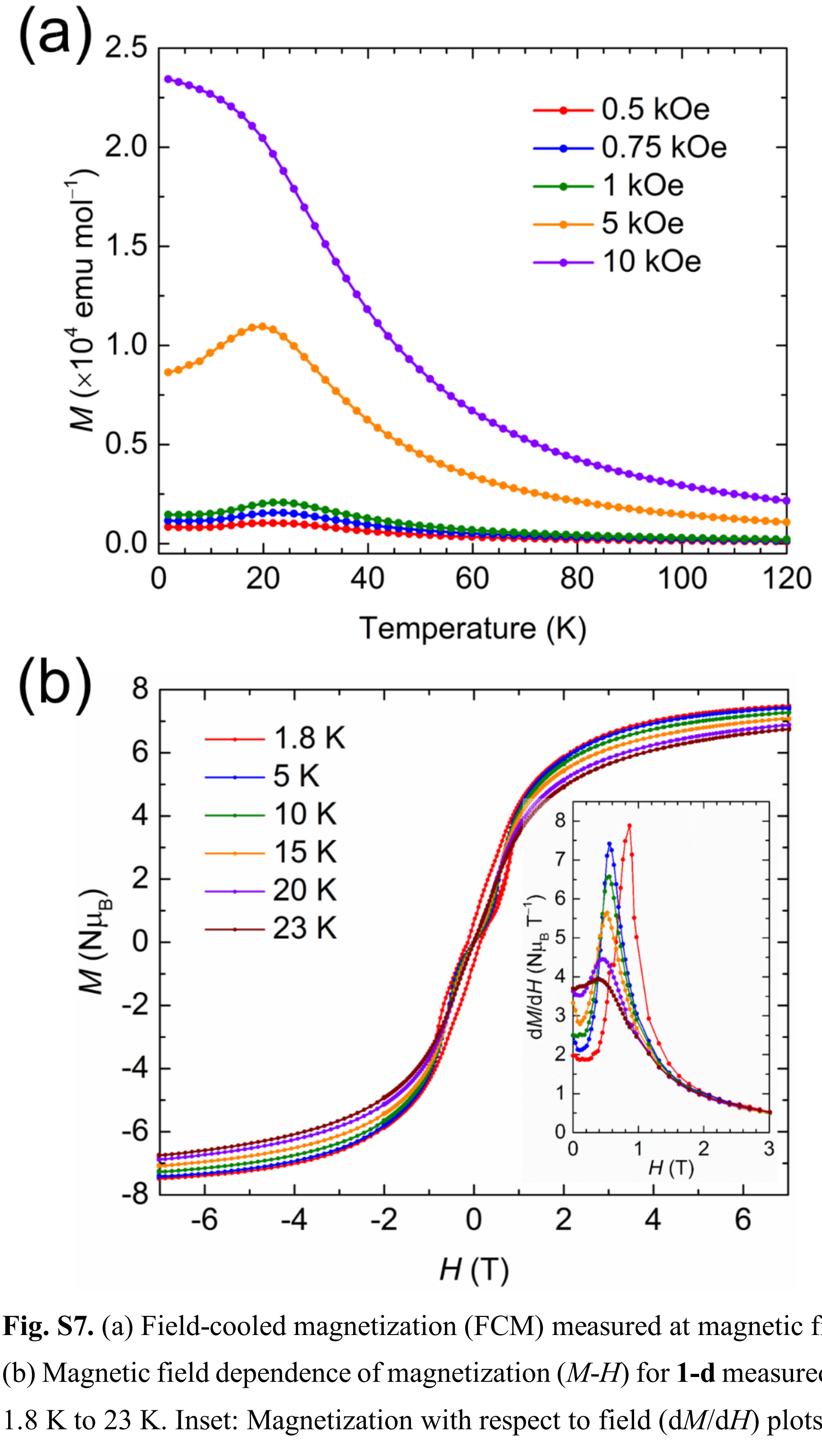

Fig. S7. (a) Field-cooled magnetization (FCM) measured at magnetic fields from 0.5 kOe to 10 kOe. (b) Magnetic field dependence of magnetization (M-H) for **1-d** measured at several temperatures from 1.8 K to 23 K. Inset: Magnetization with respect to field (dM/dH) plots for **1-d**.

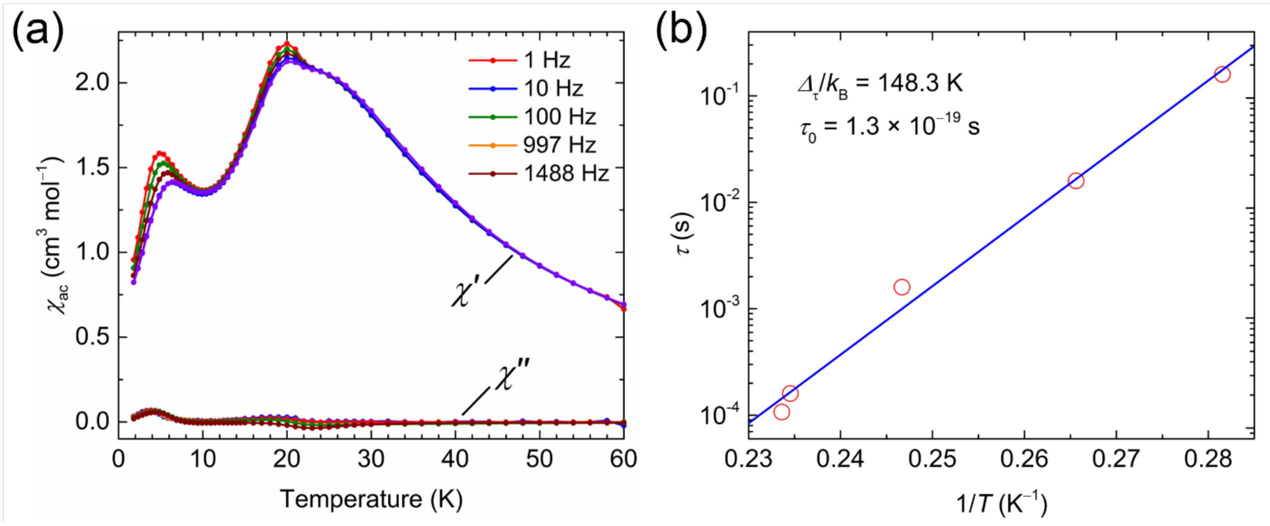

Fig. S8. (a) Temperature dependence of χ' and χ'' for **1-d** measured at H_{dc} = 0 Oe and H_{ac} = 3 Oe at several frequencies ranging from 1 Hz to 1488 Hz. (b) Arrhenius plots for **1-d** made from peak maxima in χ'' versus υ plots at H_{dc} = 0 Oe and H_{ac} = 3 Oe.

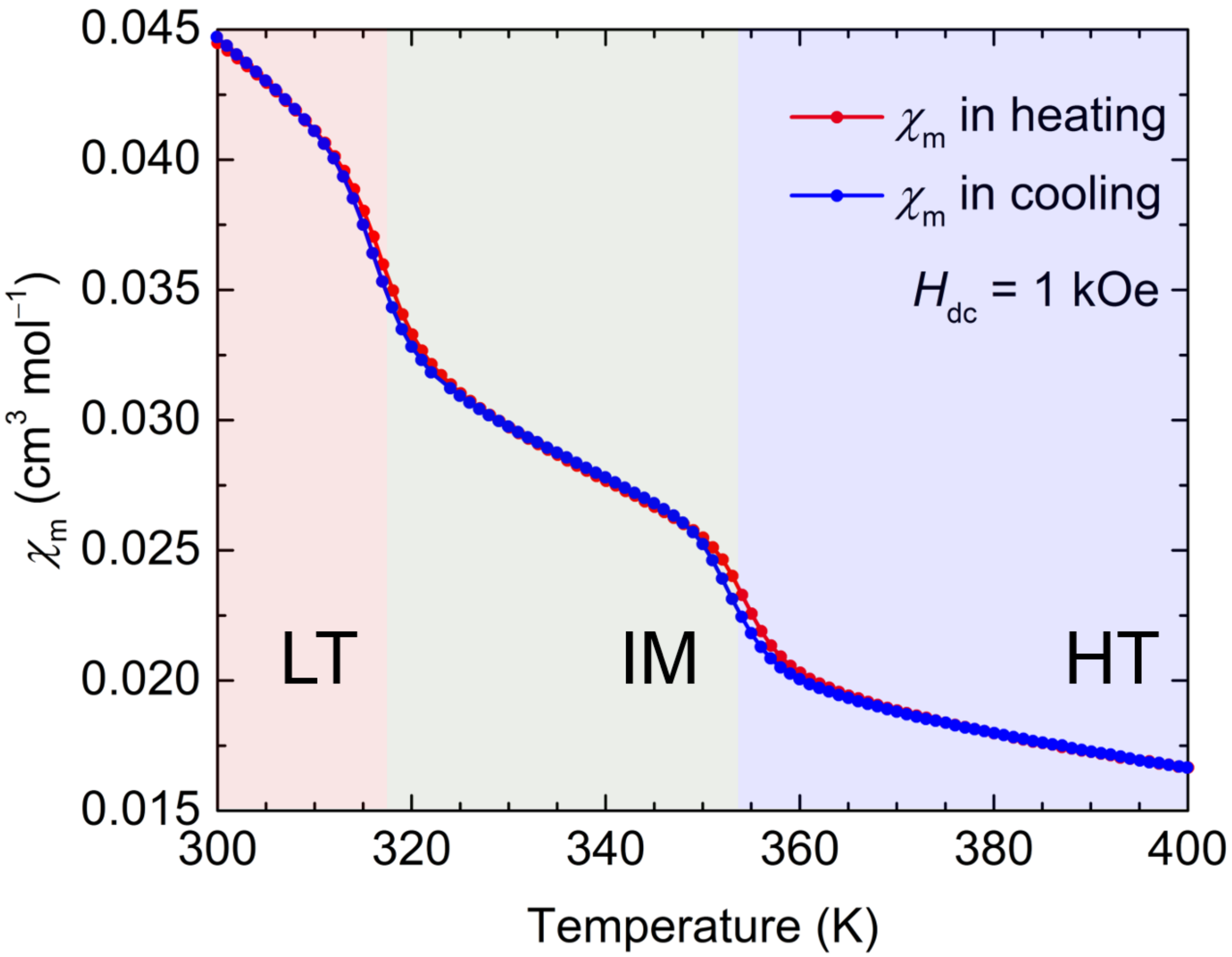

Fig. S9. Temperature dependence of χ_m for **1-d** measured at H_{dc}= 1 kOe between 300 K and 400 K, where the data recorded during cooling and heating are shown in blue and red, respectively. The pale-red (LT phase), pale-green (IM phase), and pale-blue bands (HT phase) and solid lines are highlighted guides for the eye.

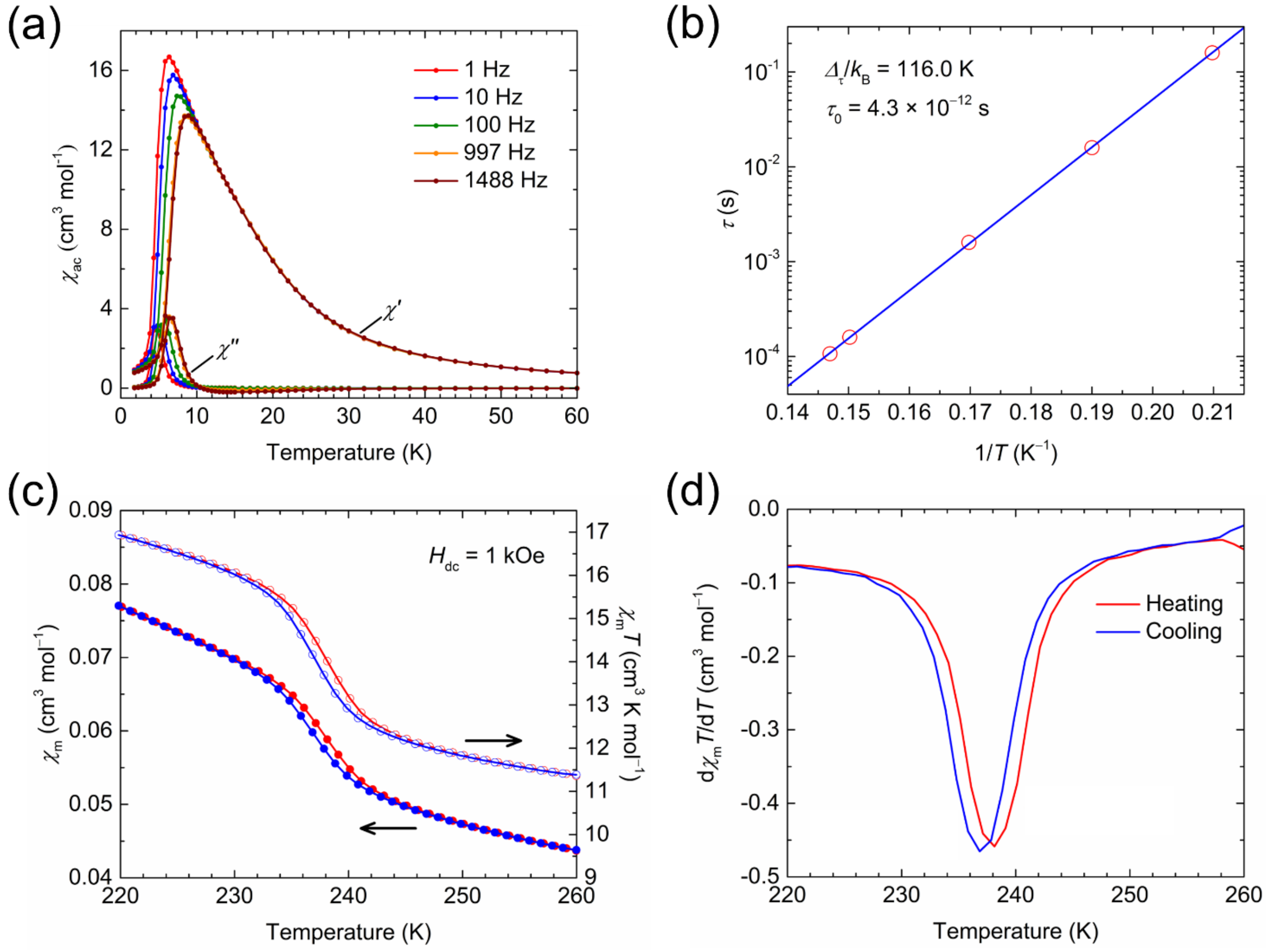

Fig. S10. Magnetic properties of **1’**. (a) Temperature dependence of χ’ and χ” for **1’** measured at H_{dc} = 0 Oe and H_{ac} = 3 Oe at several frequencies ranging from 1 Hz to 1488 Hz. (b) Arrhenius plots for **1’** made from peak maxima in χ” versus υ plots. The characteristic parameters indicate that **1’** showed single-chain magnet (SCM) behavior similar to **1**.[1,5] (c) Temperature dependence of χ_m and $\chi_m T$ for **1’** measured at H_{dc}= 1 kOe between 220 K and 260 K. The colored solid lines are a guide for the eye. (d) Temperature dependence of the derivative of $\chi_m T$ for **1’** with respect to temperature. **1’** exhibits a significant step in the χ_m and $\chi_m T$ values caused by electron transfer at $T_{1/2a}$.

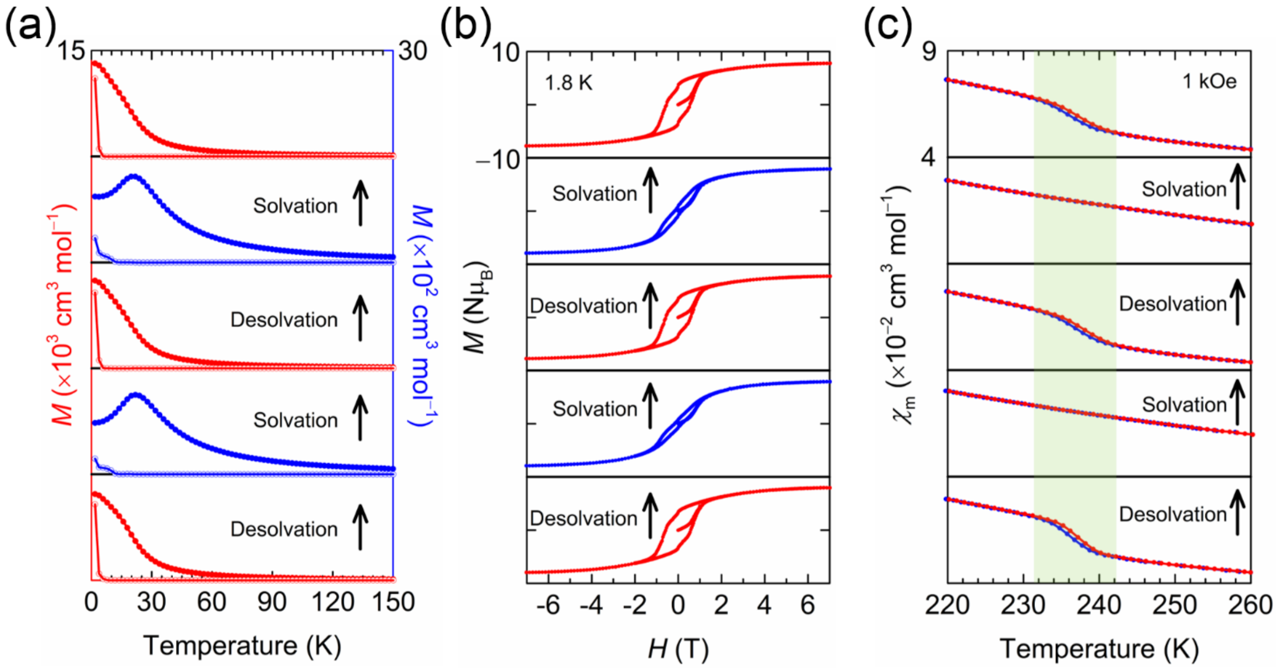

Fig. S11. Magnetic properties variation in desolvation/solvation cycles in *ex situ* magnetic measurements. (a) Variation of magnetization in the desolvation/solvation cycles. The closed and open circles represent the field-cooled magnetization (FCM) measured by applying H_{dc} = 1 kOe and the remnant magnetization (RM), respectively. (b) Magnetic field dependence of magnetization (M-H) at 1.8 K for solvated and desolvated phases in the cycling procedure. (c) Temperature dependence of χ_m measured at H_{dc} = 1 kOe between 220 K and 260 K in the desolvation/solvation cycles, where the data recorded during heating and cooling are represented by closed and open circles, respectively. The χ_m-T curves around $T_{1/2a}$ are highlighted by pale-green band.

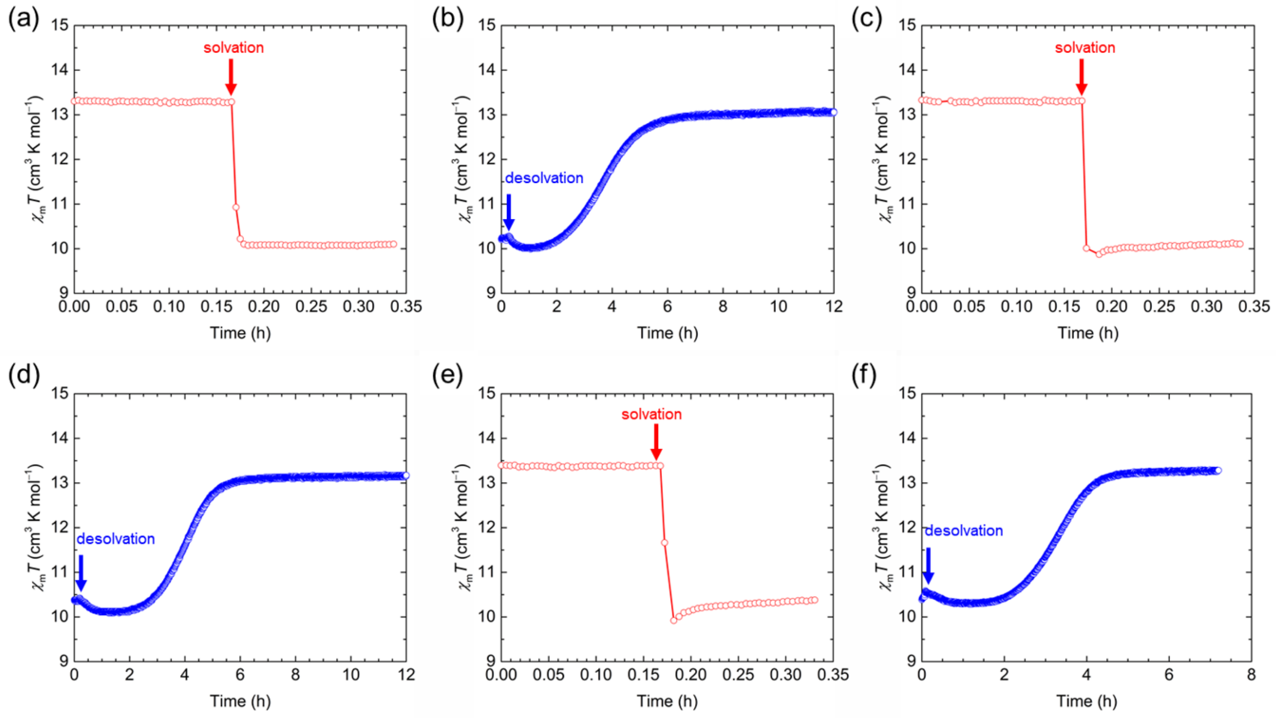

Fig. S12. Time course of the magnetic data by solvation/desolvation process *in situ* magnetic experiments. (a), (c), and (e) represent 1st, 2nd, and 3rd solvation process. (b), (d) and (f) represent 1st, 2nd, and 3rd desolvation process.

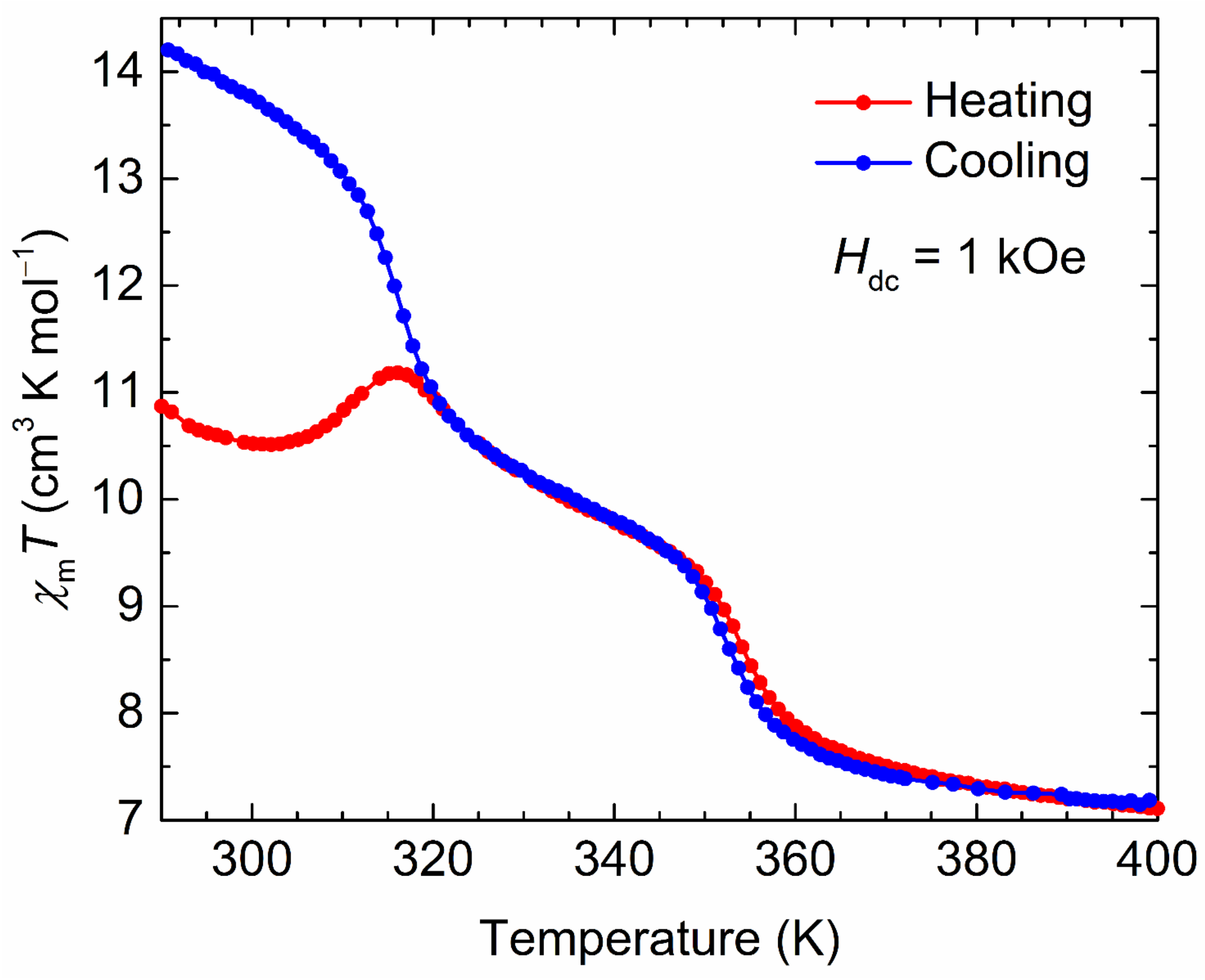

Fig. S13. Temperature dependence of $\chi_m T$ value of **1** with sweep mode (0.5 K min^{-1}). The temperature variation profile was followed as bellow: (i) heating (red circles) from 290 K to 400 K, (ii) cooling (blue circles) from 400 K to 290 K. The variation of $\chi_m T$ from 305 K to 316 K in heating process indicates the transformation of material state from IM_o (**1**) to IM_o (**1-d**).

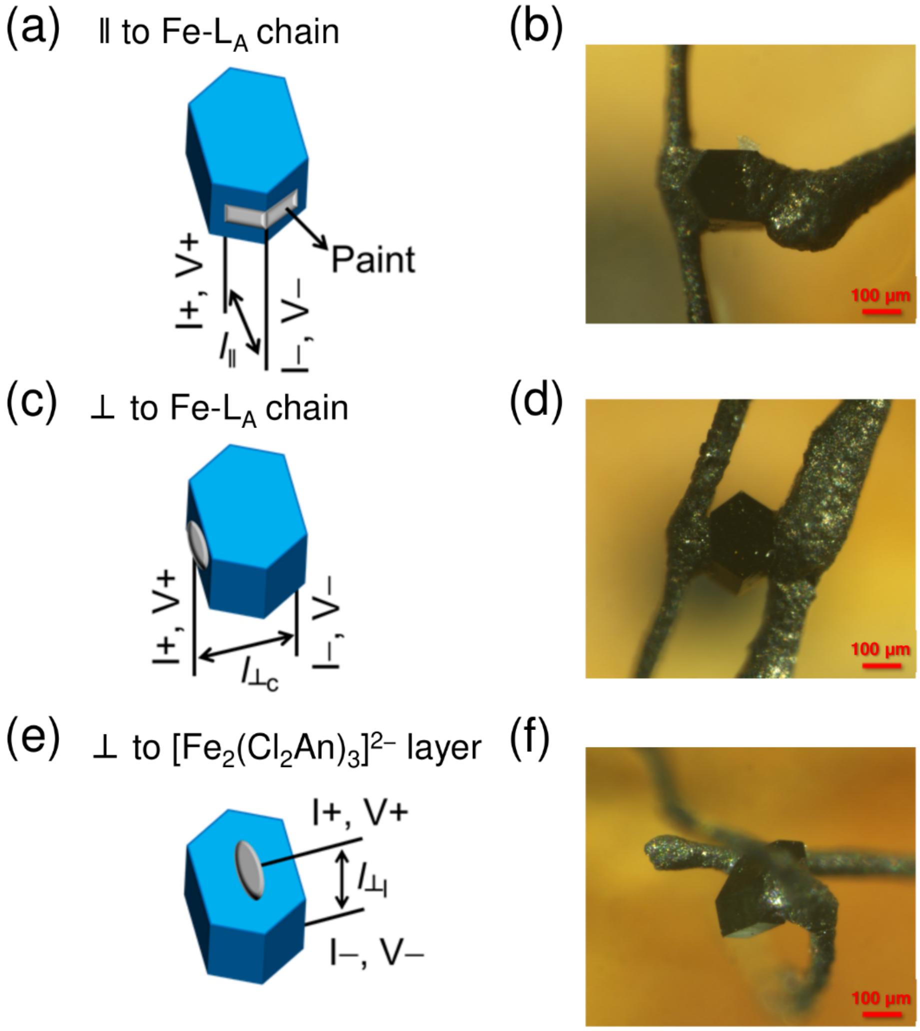

Fig. S14. Probe configurations for single crystal electronic conductivity measurements for **1-d**. (a, c, e) The illustrations of the configurations using two probes along the parallel (∥), perpendicular ($\perp_c$) to the Fe–L$_A$ chain, and perpendicular ($\perp_l$) to the $[Fe_2(Cl_2An)_3]^{2-}$ layer direction, respectively. (b, d, f) The photograph of crystals for the electronic conductivity measurements, corresponding to the illustrations of (a), (c), and (e), respectively.

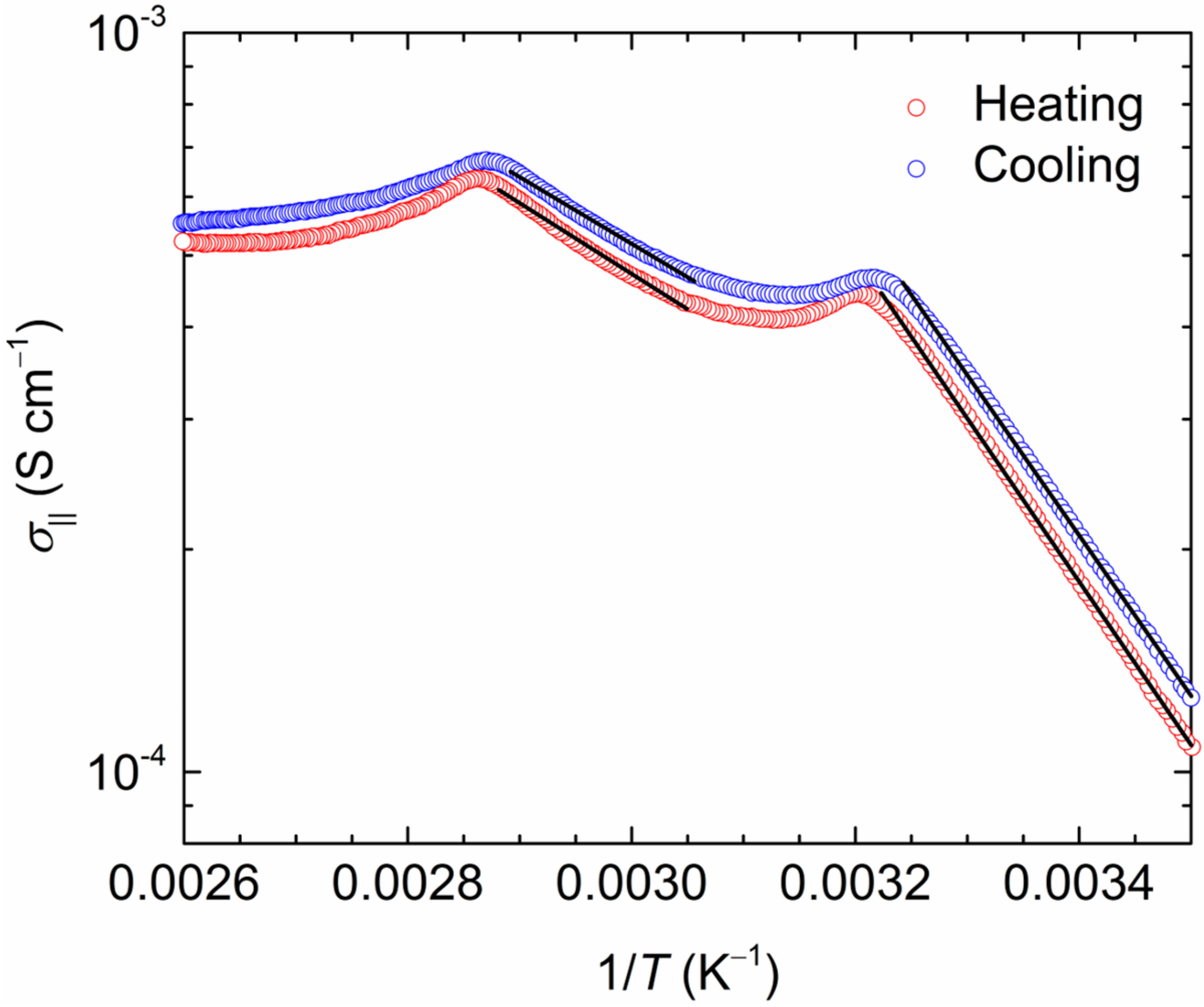

Fig. S15. Arrhenius plots of electronic conductivity data ($\sigma_{||}$) for **1-d**, where the data recorded during cooling and heating are shown in blue and red, respectively. The black lines correspond to Arrhenius fits of the data. The activation energy (E_a) for the semiconducting behavior in the LT phase and the IM$_o$ phase in the cooling process is 430.5 meV (285 K–308 K) and 179.2 meV (327 K–346 K), respectively (see in text for heating process).

References in SI

1 J. Chen, Y. Sekine, Y. Komatsumaru, S. Hayami and H. Miyasaka, *Angew. Chem. Int. Ed.*, 2018, **57**, 12043−12047.

2 G. M. Sheldrick, *Acta Cryst.*, 2008, **A64**, 112−122.

3 G. Evrard, F. Mareuil, F. Bontems, C. Sizun and J. Perez, *J. Appl. Cryst.*, 2011, **44**, 1264−1271.

4 W. Kosaka, Y. Takahashi, M. Nishio, K. Narushima, H. Fukunaga and H. Miyasaka, *Adv. Sci.*, 2018, **5**, 1700526.

5 J. A. DeGayner, K. Y. Wang and T. D. Harris, *J. Am. Chem. Soc.*, 2018, **140**, 6550−6553.